
Sample-Efficient Deep Reinforcement Learning via Episodic Backward Update

Su Young Lee

Sungik Choi

Sae-Young Chung

School of Electrical Engineering,
Korea Advanced Institute of Science and Technology,
Daejeon, Republic of Korea
{sy9424, si_choi, chung} @kaist.ac.kr

Abstract

We propose Episodic Backward Update – a new algorithm to boost the performance of a deep reinforcement learning agent by a fast reward propagation. In contrast to the conventional use of the experience replay with uniform random sampling, our agent samples a whole episode and successively propagates the value of a state to its previous states. Our computationally efficient recursive algorithm allows sparse and delayed rewards to propagate efficiently through all transitions of a sampled episode. We evaluate our algorithm on 2D MNIST Maze environment and 49 games of the Atari 2600 environment and show that our method improves sample efficiency with a competitive amount of computational cost.

1 Introduction

Recently, deep reinforcement learning (RL) has been very successful in many complex environments such as the Arcade Learning Environment (Bellemare et al., 2013) and Go (Silver et al., 2016). Deep Q-Network(DQN) algorithm (Mnih et al., 2015) with the help of experience replay (Lin, 1991 & 1992) enjoys a more stable and sample-efficient learning process, and so is able to achieve super-human performances on many tasks. Unlike simple online reinforcement learning, the use of experience replay with random sampling is known to break down the strong ties between correlated transitions. Also, experience replay allows transitions to be reused multiple times throughout the training process.

Although DQN has shown impressive achievements, it is still impractical in terms of data efficiency. To achieve a human-level performance in the Arcade Learning Environment, DQN requires 200 million frames of experience for training, which is approximately 39 days of game play in real time. Recall that it usually takes no more than a couple of hours for a skilled human player to get used to such games. In this sense, we notice that there is still a tremendous gap between the learning process of a human and that of a deep reinforcement learning agent. This problem is even more crucial in environments such as autonomous driving, where we cannot risk many trials and errors due to the high cost of samples.

One of the reasons that DQN suffers from such low sample efficiency could be the sampling method over the replay memory. In many practical problems, the agent observes sparse and delayed reward signals. There are two problems when we sample one-step transitions uniformly at random from the replay memory. (1) We have a very low chance of sampling transitions with rewards for their sparsity. The transitions with rewards should always be updated, otherwise the agent cannot figure out which action maximizes its expected return in such situations. (2) In the early stages of training, when all values are initialized to zero, there is no point in updating values of one-step transitions with zero rewards if the values of future transitions with nonzero rewards have not been updated yet. Without

the future reward signals propagated, the sampled transition will always be trained to return a zero value.

In this work, we propose Episodic Backward Update (EBU) to present solutions for such problems. Our idea originates from a naïve human strategy to solve such RL problems. When we observe an event, we scan through our memory and seek for another event that has led to the former one. Such episodic control method is how humans normally recognize the cause and effect relationship (Lengyel & Dayan, 2007). We can take a similar approach to train an RL agent. We can solve the first problem (1) by sampling transitions in an episodic manner. Then, we can be assured that at least one transition with a non-zero reward is used for the value update. We can solve the second problem (2) by updating values of transitions in a backward manner in which the transitions were made. Afterwards, we can perform an efficient reward propagation without any meaningless updates. This method faithfully follows the principle of dynamic programming.

We evaluate our update algorithm on 2D MNIST Maze Environment and the Arcade Learning Environment. We observe that our algorithm outperforms other baselines in many of the environments with a notable amount of performance boosts.

2 Related Works

Reinforcement learning deals with environments where an agent can make a sequence of actions and receive corresponding reward signals, such as Markov decision processes (MDPs). At time t , the agent encounters a state s_t , takes an action $a_t \in \mathcal{A}$, observes a next state s_{t+1} , and receives a reward $r_t \in \mathcal{R}$. The agent’s goal is to set up a policy π to take a sequence of actions so that the agent can maximize its expected return, which is the expected value of the discounted sum of rewards $\mathbb{E}_\pi[\sum_t \gamma^t r_t]$.

Q-learning (Watkins, 1989) is one of the most widely used methods to solve such RL tasks. The key idea of Q-learning is to estimate the state-action value function $Q(s, a)$, generally called as the Q-function. The state-action value function may be characterized by the Bellman optimality equation

$$Q^*(s_t, a) = \mathbb{E}[r_t + \gamma \max_{a'} Q^*(s_{t+1}, a')]. \quad (1)$$

Given the state-action value function $Q(s, a)$, the agent may perform the best action $a^* = \operatorname{argmax}_a Q(s, a)$ at each time step to maximize the expected return.

There are two major inefficiencies in the traditional Q-learning. First, each experience is used only once to update the Q-network. Secondly, learning from experiences in a chronologically forward order is much more inefficient than learning in a chronologically backward order. Experience replay (Lin, 1991 & 1992) is proposed to overcome these inefficiencies. After observing a transition (s_t, a_t, r_t, s_{t+1}) , the agent stores the transition into its replay buffer. In order to learn the Q-values, the agent samples transitions from the replay in a backward order.

In practice, the state space is extremely large, so it is impractical to tabularize Q-values of all state-action pairs. Deep Q-Network (Mnih et al., 2015) overcomes this issue by using deep neural networks to approximate the Q-function. Deep Q-Network (DQN) takes a 2D representation of a state s_t as an input. Then the information of the state s_t passes through a number of convolutional neural networks (CNNs) and fully connected networks. Then it finally returns the Q-values of each action a_t at state s_t . DQN adopts experience replay to use each transition in multiple updates. Since DQN uses a function approximator, consecutive states output similar Q-values. If DQN updates transitions in a chronologically backward order, often errors cumulate and degrade the performance. Therefore, DQN does not sample transitions in a backward order, but uniformly at random to train the network. This process breaks down the correlations between consecutive transitions and reduces the variance of updates.

There have been a variety of methods proposed to improve the performance of DQN in terms of stability, sample efficiency and runtime. Some methods propose new network architectures. The dueling network architecture (Wang et al., 2016) contains two streams of separate Q-networks to estimate the value functions and the advantage functions. Neural episodic control (Pritzel et al., 2017) and model free episodic control (Blundell et al., 2016) use episodic memory modules to estimate the state-action values.

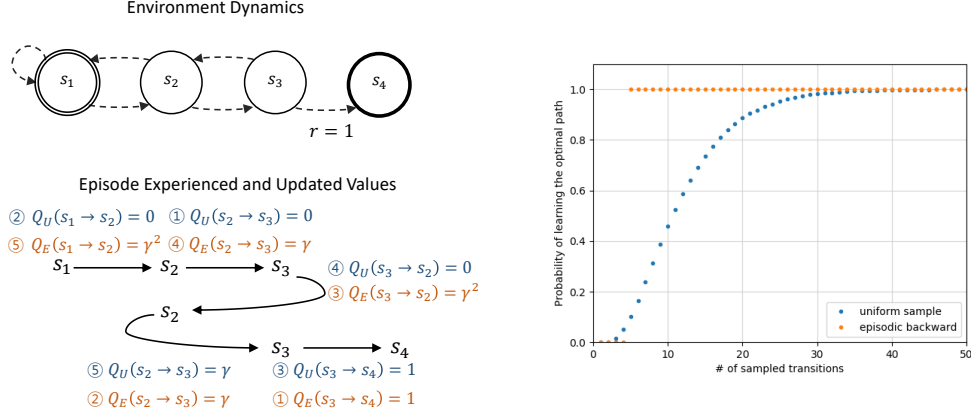


Figure 1: A motivating example where uniform sampling method fails but EBU does not. **Left:** A simple navigation domain with 4 states and a single rewarded transition. Circled numbers indicate the order of sample updates. Q_U and Q_E stand for the Q-values learned by the uniform sampling method and EBU method respectively. **Right:** The probability of learning the optimal path ($s_1 \rightarrow s_2 \rightarrow s_3 \rightarrow s_4$) after updating the Q-values with sample transitions.

Some methods tackle the uniform random sampling replay strategy of DQN. Prioritized experience replay (Schaul et al., 2016) assigns non-uniform probability to sample transitions, where greater probability is assigned for transitions with higher temporal difference error.

Inspired by Lin’s backward use of replay memory, some methods try to aggregate TD values with Monte-Carlo returns. $Q(\lambda)$ (Watkins & Dayan, 1992), $Q^*(\lambda)$ (Harutyunyan et al., 2016) and Retrace(λ) (Munos et al., 2016) modify the target values to allow the on-policy samples to be used interchangeably for on-policy and off-policy learning. Count-based exploration method combined with intrinsic motivation (Bellemare et al., 2016) takes a mixture of one-step return and Monte-Carlo return to set up the target value. Optimality Tightening (He et al., 2017) applies constraints on the target using the values of several neighboring transitions. Simply by adding a few penalty terms into the loss, it efficiently propagates reliable values to achieve faster convergence.

Our work lies on the same line of research. Without a single change done on the network structure of the original DQN, we only modify the target generation method. Instead of using a limited number of consecutive transitions, our method samples a whole episode from the replay memory and propagates values sequentially throughout the entire sampled episode in a backward manner. By using a temporary backward Q-table with a diffusion coefficient, our novel algorithm effectively reduces the errors generated from the consecutive updates of correlated states.

3 Episodic Backward Update

We start with a simple motivating toy example to describe the effectiveness of Episodic Backward Update. Then we generalize the idea into deep learning architectures and propose a full algorithm.

3.1 Motivation

Let us imagine a simple graph environment with a sparse reward (Figure 1, up) where an agent can only take two actions, left or right. In this example, s_1 is the initial state and s_4 is the terminal state. A reward of 1 is gained only when the agent moves to the terminal state and a reward of 0 is gained from any other transitions. To make it simple, assume that we only have one episode stored in the experience memory: ($s_1 \rightarrow s_2 \rightarrow s_3 \rightarrow s_2 \rightarrow s_3 \rightarrow s_4$). The Q-values of all transitions are initialized to zero. When sampling transitions uniformly at random as Nature DQN, the key transitions ($s_1 \rightarrow s_2$), ($s_2 \rightarrow s_3$) and ($s_3 \rightarrow s_4$) may not be sampled for updates. Even when those transitions are sampled, there is no guarantee that the update of the transition ($s_3 \rightarrow s_4$) is done before the update of ($s_2 \rightarrow s_3$). We can speed up the reward propagation by updating all transitions within the episode in a backward manner. Such recursive update is also computationally efficient.

Algorithm 1 Simple Episodic Backward Update (single episode, tabular)

- 1: Initialize the Q- table $Q \in \mathbb{R}^{\mathcal{S} \times \mathcal{A}}$ with zero matrix.
 $Q(s, a) = 0$ for all state action pairs $(s, a) \in \mathcal{S} \times \mathcal{A}$.
 - 2: Experience an episode $E = \{(s_1, a_1, r_1, s_2), \dots, (s_T, a_T, r_T, s_{T+1})\}$
 - 3: **for** $t = T$ to 1 **do**
 - 4: $Q(s_t, a_t) \leftarrow r_t + \gamma \max_{a'} Q(s_{t+1}, a')$
 - 5: **end for**
-

We can calculate the probability of learning the optimal path ($s_1 \rightarrow s_2 \rightarrow s_3 \rightarrow s_4$) as a function of the number of sample transitions trained. With simple Episodic Backward Update stated in Algorithm 1, which is a special case of Lin’s algorithm (Lin, 1991) with recency parameter $\lambda = 0$, the agent can figure out the optimal policy just after 5 updates of Q-values. However, we see that the uniform sampling method requires more than 40 transitions to learn the optimal path (Figure 1, down).

Note that this method differs from the standard n-step Q-learning (Watkins, 1989).

$$Q(s_t, a_t) \leftarrow (1 - \alpha)Q(s_t, a_t) + \alpha(r_t + \gamma r_{t+1} + \dots + \gamma^{n-1} r_{t+n-1} + \max_a \gamma^n Q(s_{t+n}, a)). \quad (2)$$

In n-step Q-learning, the number of future steps for target generation is fixed as n . However, our method considers T future values, where T is the length of the sampled episode. N-step Q-learning takes max operator at the n -th step only, whereas our method takes max operator at every iterative backward step which can propagate high values faster. To avoid exponential decay of the Q-value, we set the learning rate $\alpha = 1$ within the single episode update.

There are some other multi-step methods which converge to the optimal state-action value function, such as $Q(\lambda)$ or $Q^*(\lambda)$. However, our algorithm neither cuts trace of trajectories as $Q(\lambda)$, nor requires the parameter λ to be small enough to guarantee convergence as $Q^*(\lambda)$. We present a detailed discussion for the relationship between EBU and other multi-step methods in Appendix F.

3.2 Episodic Backward Update Algorithm

Directly applying such backward update algorithm to deep reinforcement learning is known to show highly unstable results. We show that fundamental ideas of tabular version of the backward update algorithm may be applied to its deep version with just a few modifications. We use a function approximator to estimate the Q-values and generate a temporary target Q-table \tilde{Q} of the sampled episode for the recursive backward update. The full algorithm introduced in Algorithm 2 closely resembles that of Nature DQN (Mnih et al., 2015). Our contributions lie in the recursive backward target generation with a diffusion coefficient β (line number 10 to line number 17 of Algorithm 2), which prevents the errors from correlated states cumulating.

Our algorithm has its novelty starting from the sampling stage. Instead of sampling transitions at uniformly random, we make use of all transitions within the sampled episode $E = \{\mathcal{S}, \mathcal{A}, \mathcal{R}, \mathcal{S}'\}$. Let the sampled episode start with a state S_1 and contain T transitions. Then E can be denoted as a set of four length- T vectors: $\mathcal{S} = \{S_1, S_2, \dots, S_T\}$; $\mathcal{A} = \{A_1, A_2, \dots, A_T\}$; $\mathcal{R} = \{R_1, R_2, \dots, R_T\}$ and $\mathcal{S}' = \{S_2, S_3, \dots, S_{T+1}\}$. The temporary target Q-table \tilde{Q} is initialized to store all the target Q-values of \mathcal{S}' for all valid actions. \tilde{Q} is an $|\mathcal{A}| \times T$ matrix which stores the target Q-values of all states \mathcal{S}' for all valid actions. Therefore, the j -th column of \tilde{Q} is a column vector that contains $\hat{Q}(S_{j+1}, a; \theta^-)$ for all valid actions a , where \hat{Q} is the target Q-function parametrized by θ^- .

Our goal is to estimate the target vector \mathbf{y} , and train the network to minimize the loss between each $Q(S_j, A_j; \theta)$ and \mathbf{y}_j for all j from 1 to T . After initialization of the temporary Q-table, we perform a recursive backward update. Adopting the backward update idea, one element $\tilde{Q}[A_{k+1}, k]$ in the k -th column of the \tilde{Q} is replaced using the next transition’s target y_{k+1} . Then y_k is estimated as the maximum value of the newly modified k -th column of \tilde{Q} . Repeating this procedure in a recursive manner until the start of the episode, we can successfully apply the backward update algorithm for a deep Q-network. The process is described in detail with a supplementary diagram in Appendix D.

When $\beta = 1$, the proposed algorithm is identical to the tabular backward algorithm stated in Algorithm 1. However, now we are using a function approximator, and updating correlated states in a

Algorithm 2 Episodic Backward Update

```

1: Initialize replay memory  $D$  to capacity  $N$ 
2: Initialize on-line action-value function  $Q$  with random weights  $\theta$ 
3: Initialize target action-value function  $\hat{Q}$  with random weights  $\theta^-$ 
4: for episode = 1 to  $M$  do
5:   for  $t = 1$  to Terminal do
6:     With probability  $\epsilon$  select a random action  $a_t$ 
7:     Otherwise select  $a_t = \operatorname{argmax}_a Q(s_t, a; \theta)$ 
8:     Execute action  $a_t$ , observe reward  $r_t$  and next state  $s_{t+1}$ 
9:     Store transition  $(s_t, a_t, r_t, s_{t+1})$  in  $D$ 
10:    Sample a random episode  $E = \{S, A, R, S'\}$  from  $D$ , set  $T = \text{length}(E)$ 
11:    Generate temporary target Q table,  $\tilde{Q} = \hat{Q}(S', \cdot; \theta^-)$ 
12:    Initialize target vector  $y = \text{zeros}(T)$ 
13:     $y_T \leftarrow R_T$ 
14:    for  $k = T - 1$  to 1 do
15:       $\tilde{Q}[A_{k+1}, k] \leftarrow \beta y_{k+1} + (1 - \beta)\tilde{Q}[A_{k+1}, k]$ 
16:       $y_k \leftarrow R_k + \gamma \max_{a \in \mathcal{A}} \tilde{Q}[a, k]$ 
17:    end for
18:    Perform a gradient descent step on  $(y - Q(S, A; \theta))^2$  with respect to  $\theta$ 
19:    Every  $C$  steps reset  $\hat{Q} = Q$ 
20:  end for
21: end for

```

sequence. As a result, we observe unreliable values with errors being propagating and compounding through recursive max operations. We solve this problem by introducing the diffusion coefficient β . By setting $\beta \in (0, 1)$, we can take a weighted sum of the newly learnt value and the pre-existing value. This process stabilizes the learning process by exponentially decreasing the error terms and preventing the compounded error from propagating. Note that when $\beta = 0$, the algorithm is identical to episodic one-step DQN.

We prove that Episodic Backward Update with a diffusion coefficient $\beta \in (0, 1)$ defines a contraction operator and converges to the optimal Q-function in finite and deterministic MDPs.

Theorem 1. *Given a finite, deterministic, and tabular MDP $M = (S, A, P, R)$, the episodic backward update algorithm in Algorithm 2 converges to the optimal Q-function w.p. 1 as long as*

- The step size satisfies the Robbins-Monro condition;
- The sample trajectories are finite in lengths l : $\mathbb{E}[l] < \infty$;
- Every (state, action) pair is visited infinitely often.

We state the proof of Theorem 1 in Appendix G.

4 Experiments

Our experiments are designed to verify the following two hypotheses: 1) EBU agent can propagate reward signals fast and efficiently in environments with sparse and delayed reward signals. 2) EBU algorithm is sample-efficient in complex domains and does not suffer from stability issues despite its sequential updates of correlated states. To investigate these hypotheses, we performed experiments on 2D MNIST Maze Environment and on 49 games of the Arcade Learning Environment (Bellemare et al., 2013).

4.1 2D MNIST Maze Environment

We test our algorithm in 2D maze environment with sparse and delayed rewards. Starting from the initial position, the agent has to navigate through the maze to discover the goal position. The agent has 4 valid actions: up, down, left and right. When the agent bumps into a wall, then the agent returns

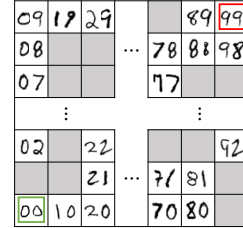


Figure 2: 2D MNIST maze

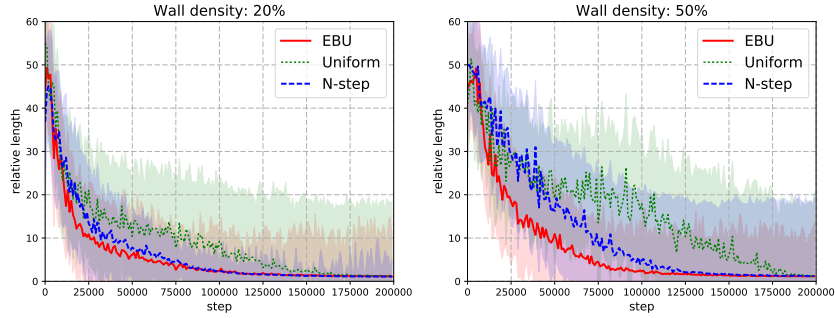


Figure 3: Median relative lengths of EBU and other baseline algorithms. As the wall density increases, EBU outperforms other baselines more significantly. The filled regions indicate the standard deviation of results from 50 random mazes.

Table 1: Relative lengths (Mean & Median) on MNIST Maze after 100,000 steps of training.

Wall density	EBU (ours)		Uniform		N-step	
20%	5.44	2.42	14.40	9.25	3.26	2.24
30%	8.14	3.03	25.63	21.03	8.88	3.32
40%	8.61	2.52	25.45	22.71	8.96	3.50
50%	5.51	2.27	22.36	17.90	11.32	4.93

to its previous state. To show effectiveness in complex domains, we use the MNIST dataset (LeCun et al., 1998) for state representation (illustrated in Figure 2). When the agent arrives at each state, it receives the coordinates of the position in two MNIST images as the state representation.

We compare the performance of EBU to uniform random sampling one-step Q-learning and n-step Q-learning. For n-step Q-learning, we set the value of n as the length of the episode. We use 10 by 10 mazes with randomly placed walls. The agent starts at (0,0) and has to reach the goal position at (9,9) as soon as possible. Wall density indicates the probability of having a wall at each position. We assign a reward of 1000 for reaching the goal and a reward of -1 for bumping into a wall. For each wall density, we generate 50 random mazes with different wall locations. We train a total of 50 independent agents, one agent for one maze over 200,000 steps each. MNIST images for a state representation are randomly selected every time the agent visits each state. The relative length is defined as $l_{rel} = l_{agent}/l_{oracle}$, which is the ratio between the length of the agent’s path l_{agent} and the length of the ground truth shortest path l_{oracle} . Figure 9 shows the median relative lengths of 50 agents over 200,000 training steps. Since all three algorithms achieve median relative lengths of 1 at the end of training, we report the mean and the median relative lengths at 100,000 steps in Table 1. For this example, we set the diffusion coefficient $\beta = 1$. The details of hyperparameters and the network structure are described in Appendix C.

The result shows that EBU agent outperforms other baselines in most of the situations. Uniform sampling DQN shows the worst performance in all configurations, implying the inefficiency of uniform sampling update in environments with sparse and delayed rewards. As the wall density increases, valid paths to the goal become more complicated. In other words, the oracle length l_{oracle} increases, so it is important for the agent to make correct decisions at bottleneck positions. N-step Q-learning shows the best performance with a low wall density, but as the wall density increases, EBU shows better performance than n-step Q. Especially when the wall density is 50%, EBU finds paths twice shorter than those of n-step Q. This performance gap originates from the difference between the target generation methods of the two algorithms. EBU performs recursive max operations at each positions, so the optimal Q-values at bottlenecks are learned faster.

4.2 Arcade Learning Environment

The Arcade Learning Environment (Bellemare et al., 2013) is one of the most popular RL benchmarks for its diverse set of challenging tasks. The agent receives high-dimensional raw observations from

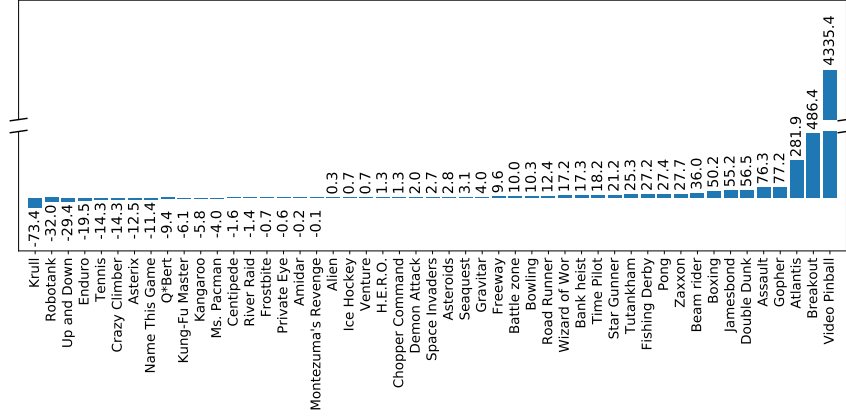


Figure 4: Relative score of EBU over Nature DQN in percentages (%) after 10 million frames of training.

exponentially large state space. Even more, observations and objectives of the games are completely different over different games, so the strategies to achieve a high score should also vary from game to game. Therefore, it is very hard to create a robust agent with a single set of networks and hyperparameters that can learn to play all games. We use the same set of 49 Atari 2600 games, which was evaluated in Nature DQN paper (Mnih et al., 2015).

We compare our algorithm to four baselines: Nature DQN, Optimality Tightening (He et al., 2017), Prioritized Experience Replay (Schaul et al., 2016) and Retrace(λ) (Munos et al., 2016). We train EBU and baseline agents for 10 million frames on 49 Atari games with the same network structure, hyperparameters and evaluation methods used by Nature DQN. The choice of such small number of training steps is made to investigate the sample efficiency of each algorithm (Pritzel et al., 2017; He et al., 2017). We divide the training steps into 40 epochs of 250,000 frames. At the end of each epoch, we evaluate the agent for 30 episodes using ϵ -greedy policy with $\epsilon = 0.05$. Transitions of the Arcade Learning Environment are fully deterministic. In order to give a diversity in experience, both train and test episodes start with at most 30 no-op actions. We train each game for 8 times with different random seeds. For each agent with a different random seed, the best evaluation score during training is taken as its result. Then we report the mean score¹ of the 8 agents as the result of the game. Detailed specifications for each baseline are described in Appendix C.

We observe that the choice of $\beta = 1$ degrades the performance in most of the games. Instead, we use $\beta = \frac{1}{2}$, which shows the best performance among $\{\frac{1}{3}, \frac{1}{2}, \frac{2}{3}, \frac{3}{4}, 1\}$ that we tried. Further fine-tuning of β may lead to a better result.

First, we show the improvement of EBU over Nature DQN for all 49 games in Figure 4. To compare the performance of an agent to its baseline’s, we use the following relative score, $\frac{\text{Score}_{\text{Agent}} - \text{Score}_{\text{Baseline}}}{\max\{\text{Score}_{\text{Human}}, \text{Score}_{\text{Baseline}}\} - \text{Score}_{\text{Random}}}$ (Wang et al., 2015). This measure shows how well an agent performs a task compared to its level of difficulty. Out of the 49 games, our agent shows better performance in 32 games. Not only that, for games such as ‘Atlantis’, ‘Breakout’ and ‘Video Pinball’, our agent shows significant improvements.

In order to compare the overall performance of an algorithm, we use the human-normalized score $\frac{\text{Score}_{\text{Agent}} - \text{Score}_{\text{Random}}}{|\text{Score}_{\text{Human}} - \text{Score}_{\text{Random}}|}$ (van Hasselt et al., 2015). We report the mean and the median of the human normalized scores of the 49 games in Table 2 and in Appendix A. The result shows that our algorithm outperforms the baselines in both mean and median of the human normalized scores. Prioritized experience replay and retrace(λ) algorithms are known to outperform Nature DQN when trained over many training steps as 200M frames. However, they do not show much improvements for a small number of training steps as 10 million frames. The result signifies the sample-efficiency of EBU algorithm in the early stages of training with a small number of training samples. Furthermore,

¹Optimality tightening reports the score of the best performing agent, whereas our experiment reports the mean score of 8 agents. The performance of OT in our paper may vary from that of He et al., 2017.

our method requires only about 37% of computation time used by Optimality Tightening. Since Optimality Tightening has to calculate the Q-values of neighboring states and compare them to generate the penalty term, it requires about 3 times more training time than Nature DQN. However, EBU performs iterative episodic updates using the temporary Q-table that is shared by all transitions in the episode, EBU has almost the same computational cost as that of Nature DQN. Raw scores for each game after 10 million frames of training are summarized in Appendix B.

Table 2: Summary of training time and human-normalized performance. Training time refers to the total time required to train 49 games of 10M frames each (490M frames in total).

	Training Time (49 games)	Mean	Median
EBU (10M)	152 hours	255.19%	53.65%
Nature DQN (10M)	138 hours	133.95%	40.42%
Optimality Tightening (10M)	407 hours	162.66%	49.42%
Prioritized Experience Replay (10M)	146 hours	156.57%	40.86%
Retrace(λ) (10M)	154 hours	93.77%	41.99%

We show the performance of EBU and the baselines for 4 games ‘Assault’, ‘Breakout’, ‘Gopher’ and ‘Video Pinball’ in Figure 5. EBU with a diffusion coefficient $\beta = 0.5$ shows competitive performances in all 4 games, reflecting that our algorithm does not suffer from the stability issue caused by the sequential update of correlated states. Other baselines fail in some games, whereas our algorithm shows stable learning processes throughout all games. Out of 49 games, our algorithm shows the worst performance in only 6 games. Such stability leads to the best median and mean scores in total. Note that naive backward algorithm with $\beta = 1.0$ fails in most games. We present the in-depth analysis of the failure of EBU with $\beta = 1.0$ in Appendix E.

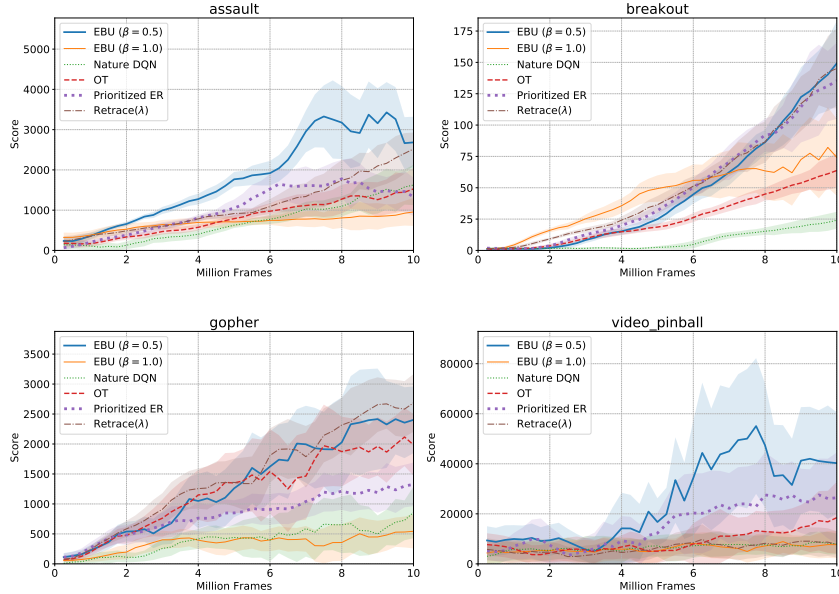


Figure 5: Scores of EBU and baselines on 4 games: ‘Assault’, ‘Breakout’, ‘Gopher’ and ‘Video Pinball’. Moving average test scores of 40 epochs with a window size 4 are plotted.

5 Conclusion

We propose Episodic Backward Update, which samples transitions episode by episode and updates values recursively in a backward manner. Our algorithm achieves fast and stable learning due to the efficient value propagation. We show that our algorithm outperforms other baselines in many complex domains without much increase in its computational cost. We do not change any network structures,

hyperparameters and exploration methods from Nature DQN. So we hope that we can make further improvements by scheduling parameters and combining other successful deep Q-learning algorithms.

References

- Bellemare, M. G., Naddaf, Y., Veness, J., and Bowling, M. The arcade learning environment: An evaluation platform for general agents. *Journal of Artificial Intelligence Research*, 47:253-279, 2013.
- Bellemare, M. G., Srinivasan, S., Ostrovski, G., Schaul, T., Saxton, D., and Munos, R. Unifying count-based exploration and intrinsic motivation. In *Advances in Neural Information Processing Systems (NIPS)*, 1471-1479, 2016.
- Bertsekas, D. P., and Tsitsiklis, J. N. *Neuro-Dynamic Programming*. Athena Scientific, 1996. Blundell, C., Uria, B., Pritzel, A., Li, Y., Ruderman, A., Leibo, J. Z., Rae, J., Wierstra, D., and Hassabis, D. Model-free episodic control. *arXiv preprint arXiv:1606.04460*, 2016.
- Harutyunyan, A., Bellemare, M. G., Stepleton, T., and Munos, R. $Q(\lambda)$ with off-policy corrections. In *International Conference on Algorithmic Learning Theory (ALT)*, 305-320, 2016.
- He, F. S., Liu, Y., Schwing, A. G., and Peng, J. Learning to play in a day: Faster deep reinforcement learning by optimality tightening. In *International Conference on Learning Representations (ICLR)*, 2017.
- LeCun, Y., Bottou, L., Bengio, Y., and Haffner, P. Gradient-based learning applied to document recognition. In *Institute of Electrical and Electronics Engineers (IEEE)*, 86, 2278-2324, 1998.
- Lengyel, M., and Dayan, P. Hippocampal Contributions to Control: The Third Way. In *Advances in Neural Information Processing Systems (NIPS)*, 889-896, 2007.
- Lin, L.-J. Programming Robots Using Reinforcement Learning and Teaching. In *Association for the Advancement of Artificial Intelligence (AAAI)*, 781-786, 1991.
- Lin, L.-J. Self-improving reactive agents based on reinforcement learning, planning and teaching. *Machine Learning*, 293-321, 1992.
- Melo, F. S. Convergence of Q-learning: A simple proof, Institute Of Systems and Robotics, Tech. Rep, 2001.
- Mnih, V., Kavukcuoglu, K., Silver, D., Rusu, A. A., Veness, J., Bellemare, M. G., Graves, A., Riedmiller, M., Fidjeland, A. K., Ostrovski, G., Petersen, S., Beattie, C., Sadik, A., Antonoglou, I., King, H., Kumaran, D., Wierstra, D., Legg, S., and Hassabis, D. Human-level control through deep reinforcement learning. *Nature*, 518(7540):529-533, 2015.
- Munos, R., Stepleton, T., Harutyunyan, A., and Bellemare, M. G. Safe and efficient off-policy reinforcement learning. In *Advances in Neural Information Processing Systems (NIPS)*, 1046-1054, 2016.
- Pritzel, A., Uria, B., Srinivasan, S., Puig-domenech, A., Vinyals, O., Hassabis, D., Wierstra, D., and Blundell, C. Neural Episodic Control. In *International Conference on Machine Learning (ICML)*, 2827-2836, 2017.
- Schaul, T., Quan, J., Antonoglou, I., and Silver, D. Prioritized Experience Replay. In *International Conference on Learning Representations (ICLR)*, 2016.
- Silver, D., Huang, A., Maddison C. J., Guez, A., Sifre, L., van den Driessche, G., Schrittwieser, J., Antonoglou, I., Panneershelvam, V., Lanctot, M., Dieleman, S., Grewe, D., Nham, J., Kalchbrenner, N., Sutskever, I., Lillicrap, T., Leach, M., Kavukcuoglu, K., Graepel, T., and Hassabis, D. Mastering the game of Go with deep neural networks and tree search. *Nature*, 529:484-489, 2016.
- Sutton, R. S., and Barto, A. G. *Reinforcement Learning: An Introduction*. MIT Press, 1998.
- van Hasselt, H., Guez, A., and Silver, D. Deep Reinforcement Learning with Double Q-learning. In *Association for the Advancement of Artificial Intelligence (AAAI)*, 2094-2100, 2016.
- Wang, Z., Schaul, T., Hessel, M., van Hasselt, H., Lanctot, M., and de Freitas, N. Dueling Network Architectures for Deep Reinforcement Learning. In *International Conference on Machine Learning (ICML)*, 1995-2003, 2016.
- Watkins, C. J. C. H. Learning from delayed rewards. PhD thesis, University of Cambridge England, 1989.
- Watkins, C. J. C. H., and Dayan, P. Q-learning. *Machine Learning*, 272-292, 1992.

Appendix A Average performance over all 49 games

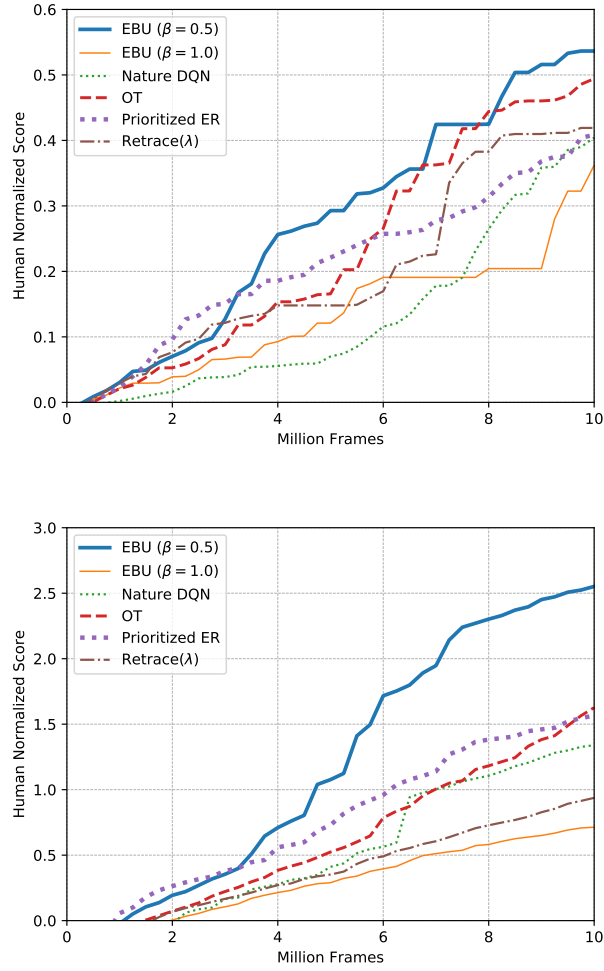


Figure 6: Learning curves of EBU and baselines on 49 games of the Arcade Learning Environment. **Up**: median over 49 games. **Down**: mean over 49 games. We use the average of 30 no-op scores of 8 agents with different random seeds. Use of different evaluation methods and seeds may output different results.

Appendix B Raw Scores of All 49 Games.

Table 3: Raw scores after 10 million frames of trainig. Mean scores from 8 random seeds are used.

	EBU	Nature DQN	OT	Retrace	Prioritized ER
Alien	708.08	690.32	1078.67	708.29	1026.96
Amidar	122.07	125.42	220.00	182.68	167.63
Assault	4109.18	2426.94	2499.23	2989.05	2720.69
Asterix	1898.12	2936.54	2592.50	1798.54	2218.54
Asteroids	1002.17	654.99	985.88	886.92	993.50
Atlantis	66271.67	20666.84	57520.00	98182.81	35665.83
Bank heist	359.62	234.70	407.42	223.50	312.96
Battle zone	26002.44	22468.75	20400.48	30128.36	20835.74
Beam rider	5628.99	3682.92	5889.54	4093.76	4586.07
Bowling	78.80	65.23	53.45	42.62	42.74
Boxing	55.95	37.28	60.89	6.76	4.64
Breakout	174.76	28.36	75.00	171.86	164.22
Centipede	6052.38	6207.30	5277.79	5986.16	4385.41
Chopper Command	1287.08	1168.67	1615.00	1353.76	1344.24
Crazy Climber	65329.63	74410.74	92972.08	64598.21	53166.47
Demon Attack	7924.14	7772.39	6872.04	6450.84	4446.03
Double Dunk	-16.19	-17.94	-15.92	-15.81	-15.62
Enduro	415.59	516.10	615.05	208.10	308.75
Fishing Derby	-39.13	-65.53	-69.66	-75.74	-78.49
Freeway	19.07	16.24	14.63	15.26	9.35
Frostbite	437.92	466.02	2452.75	825.00	536.00
Gopher	3318.50	1726.52	2869.08	3410.75	1833.67
Gravitar	294.58	193.55	263.54	272.08	319.79
H.E.R.O.	3089.90	2767.97	10698.25	3079.43	3052.04
Ice Hockey	-4.71	-4.79	-5.79	-6.13	-7.73
Jamesbond	391.67	183.35	325.21	436.25	421.46
Kangaroo	535.83	709.88	708.33	538.33	782.50
Krull	7587.24	24109.14	7468.70	6346.40	6642.58
Kung-Fu Master	20578.33	21951.72	22211.25	18815.83	18212.89
Montezuma's Revenge	1.04	3.95	0.00	0.00	0.43
Ms. Pacman	1249.79	1861.80	1849.00	1310.62	1784.75
Name This Game	6960.46	7560.33	7358.25	6094.08	5757.03
Pong	5.53	-2.68	2.60	8.65	12.83
Private Eye	953.58	1388.45	1277.53	714.97	269.28
Q*Bert	785.00	2037.21	3955.10	3192.08	1215.42
River Raid	3460.62	3636.72	4643.62	4178.92	6005.62
Road Runner	10086.74	8978.17	19081.55	9390.83	17137.92
Robotank	11.65	16.11	12.17	9.90	6.46
Seaquest	1380.67	762.10	2170.33	2275.83	1955.67
Space Invaders	797.29	755.95	869.83	783.35	762.54
Star Gunner	2737.08	708.66	1710.83	2856.67	2629.17
Tennis	-3.41	0.00	-6.37	-2.50	-10.32
Time Pilot	3505.42	3076.98	4012.50	3651.25	4434.17
Tutankham	204.83	165.27	247.81	156.16	255.74
Up and Down	6841.83	9468.04	6706.83	7574.53	7397.29
Venture	105.10	96.70	106.67	50.85	60.40
Video Pinball	84859.24	17803.69	38528.58	18346.58	55646.66
Wizard of Wor	1249.89	529.85	1177.08	1083.69	1175.24
Zaxxon	3221.67	685.84	2467.92	596.67	3928.33

Appendix C Network structure and hyperparameters

2D MNIST Maze Environment

Each state is given as a grey scale 28×28 image. We apply 2 convolutional neural networks (CNNs) and one fully connected layer to get the output Q-values for 4 actions: up, down, left and right. The first CNN uses 64 channels with 4×4 kernels and stride of 3. The next CNN uses 64 channels with 3×3 kernels and stride of 1. Then the layer is fully connected into size of 512. Then we fully connect the layer into size of the action space 4. After each layer, we apply rectified linear unit.

We train the agent for a total of 200,000 steps. The agent performs ϵ -greedy exploration. ϵ starts from 1 and is annealed to 0 at 200,000 steps in a quadratic manner: $\epsilon = \frac{1}{(200,000)^2}(\text{step} - 200,000)^2$. We use RMSProp optimizer with a learning rate of 0.001. The online-network is updated every 50 steps, the target network is updated every 2000 steps. The replay memory size is 30000 and we use minibatch size of 350. We use a discount factor $\gamma = 0.9$ and a diffusion coefficient $\beta = 1.0$. The agent plays the game until it reaches the goal or it stays in the maze for more than 1000 time steps.

Arcade Learning Environment

Common Specifications

Almost all specifications such as hyperparameters and network structures are identical for all baselines. We use exactly the same network structure and hyperparameters of Nature DQN (Mnih et al., 2015). The raw observation is preprocessed into gray scale image of 84×84 . Then it passes through three convolutional layers: 32 channels with 8×8 kernels with stride of 4; 64 channels with 4×4 kernels with stride of 2; 64 channels with 3×3 kernels with stride of 1. Then it is fully connected into size of 512. Then it is again fully connected into the size of the action space.

We train agents for 10 million frames each, which is equivalent to 2.5 million steps with frame skip of 4. The agent performs ϵ -greedy exploration. ϵ starts from 1 and is linearly annealed to reach the final value 0.1 at 4 million frames of training. To give randomness in experience, we select a number k from 1 to 30 uniform randomly at the start of each train and test episode. We start the episode with k no-op actions. The network is trained by RMSProp optimizer with a learning rate of 0.00025. At each step, we update transitions in minibatch with size 32. The replay buffer size is 1 million steps (4 million frames). The target network is updated every 10,000 steps. The discount factor is $\gamma = 0.99$.

We divide the training process into 40 epochs of 250,000 frames each. At the end of each epoch, the agent is tested for 30 episodes with $\epsilon = 0.05$. The agent plays the game until it runs out of lives or time (18,000 frames, 5 minutes in real time).

Below are detailed specifications for each algorithm.

1. Episodic Backward Update

We set the diffusion coefficient $\beta = 0.5$.

2. Optimality Tightening

We used the code (<https://github.com/ShibiHe/Q-Optimality-Tightening>) uploaded by the authors of Optimality Tightening (He et al., 2017) to evaluate the baseline. To generate the lower and upper bounds, we use 4 future transitions and 4 past transitions.

3. Prioritized Experience Replay

We use the rank-based DQN version of Prioritized ER and use the hyperparameters chosen by the authors (Schaul et al., 2016): $\alpha = 0.5 \rightarrow 0$ and $\beta = 0$.

4. Retrace(λ)

Just as EBU, we sample a random episode and then generate the Retrace target for the transitions in the sampled episode. We follow the same evaluation process as that of Munos et al., 2016. First, we calculate the trace coefficients from $s = 1$ to $s = T$ (terminal).

$$c_s = \lambda \min \left(1, \frac{\pi(a_s|x_s)}{\mu(a_s|x_s)} \right) \quad (3)$$

Where μ is the behavior policy of the sampled transition and the evaluation policy π is the current policy. Then we generate a loss vector for transitions in the sample episode from $t = T$ to $t = 1$.

$$\Delta Q(x_{t-1}, a_{t-1}) = c_t \lambda \Delta Q(x_t, a_t) + [r(x_{t-1}, a_{t-1}) + \gamma \mathbb{E}_\pi Q(x_t, :) - Q(x_{t-1}, a_{t-1})]. \quad (4)$$

Appendix D Supplementary Figure: Backward Update Algorithm

Line #10 of Algorithm 2: Sample a random episode E .

T

S	S_1	...	S_{T-2}	S_{T-1}	S_T
A	A_1	...	A_{T-2}	A_{T-1}	A_T
R	R_1	...	R_{T-2}	R_{T-1}	R_T
S'	S_2	...	S_{T-1}	S_T	S_{T+1}

Line # 11~13: Generate a temporary target Q table \tilde{Q} with the next state vector S' . Initialize a target vector y . Let there be n possible actions in the environment. $\mathcal{A} = \{a^{(1)}, a^{(2)}, \dots, a^{(n)}\}$. Note that \tilde{Q} is the target Q-value and $\tilde{Q}(S_{T+1}, \cdot) = 0$.

\tilde{Q}	$\tilde{Q}(S_2, a^{(1)})$...	$\tilde{Q}(S_{T-1}, a^{(1)})$	$\tilde{Q}(S_T, a^{(1)})$	0
	$\tilde{Q}(S_2, a^{(2)})$...	$\tilde{Q}(S_{T-1}, a^{(2)})$	$\tilde{Q}(S_T, a^{(2)})$	0
	\vdots	\vdots	\vdots	\vdots	\vdots
	$\tilde{Q}(S_2, a^{(n)})$...	$\tilde{Q}(S_{T-1}, a^{(n)})$	$\tilde{Q}(S_T, a^{(n)})$	0

n

y	0	...	0	0	R_T
-----	---	-----	---	---	-------

Line # 14~17, first iteration ($k = T-1$): Update \tilde{Q} and y . Let the T -th action in the replay memory be $A_T = a^{(2)}$.

- ① line # 15: update $\tilde{Q}[A_{k+1}, k] = \tilde{Q}[A_T, T-1] = \tilde{Q}[a^{(2)}, T-1] \leftarrow \beta y_T + (1-\beta)\tilde{Q}(S_T, a^{(2)})$
 ② line # 16: update $y_k = y_{T-1} \leftarrow R_{T-1} + \gamma \max \tilde{Q}[:, T-1]$

index	1	...	T-2	T-1	T
$a^{(1)}$	$\tilde{Q}(S_2, a^{(1)})$...	$\tilde{Q}(S_{T-1}, a^{(1)})$	$\tilde{Q}(S_T, a^{(1)})$	0
$a^{(2)}$	$\tilde{Q}(S_2, a^{(2)})$...	$\tilde{Q}(S_{T-1}, a^{(2)})$	$\beta y_T + (1-\beta)\tilde{Q}(S_T, a^{(2)})$	0
\vdots	\vdots	\vdots	\vdots	\vdots	\vdots
$a^{(n)}$	$\tilde{Q}(S_2, a^{(n)})$...	$\tilde{Q}(S_{T-1}, a^{(n)})$	$\tilde{Q}(S_T, a^{(n)})$	0

n

y	0	...	0	$R_{T-1} + \gamma \max \tilde{Q}[:, T-1]$	R_T
-----	---	-----	---	---	-------

Line # 14~17, second iteration ($k = T-2$): Update \tilde{Q} and y . Let the $(T-1)$ -th action in the replay memory be $A_{T-1} = a^{(1)}$.

- ① line # 15: update $\tilde{Q}[A_{k+1}, k] = \tilde{Q}[A_{T-1}, T-2] = \tilde{Q}[a^{(1)}, T-2] \leftarrow \beta y_{T-1} + (1-\beta)\tilde{Q}(S_{T-1}, a^{(1)})$
 ② line # 16: update $y_k = y_{T-2} \leftarrow R_{T-2} + \gamma \max \tilde{Q}[:, T-2]$

index	1	...	T-2	T-1	T
$a^{(1)}$	$\tilde{Q}(S_2, a^{(1)})$...	$\beta y_{T-1} + (1-\beta)\tilde{Q}(S_{T-1}, a^{(1)})$	$\tilde{Q}(S_T, a^{(1)})$	0
$a^{(2)}$	$\tilde{Q}(S_2, a^{(2)})$...	$\tilde{Q}(S_{T-1}, a^{(2)})$	$\beta y_T + (1-\beta)\tilde{Q}(S_T, a^{(2)})$	0
\vdots	\vdots	\vdots	\vdots	\vdots	\vdots
$a^{(n)}$	$\tilde{Q}(S_2, a^{(n)})$...	$\tilde{Q}(S_{T-1}, a^{(n)})$	$\tilde{Q}(S_T, a^{(n)})$	0

n

y	0	...	$R_{T-2} + \gamma \max \tilde{Q}[:, T-2]$	$R_{T-1} + \gamma \max \tilde{Q}[:, T-1]$	R_T
-----	---	-----	---	---	-------

Repeat this update until $k=1$.

Figure 7: Target generation process from the sampled episode E

Appendix E Role of the Diffusion Coefficient β in EBU

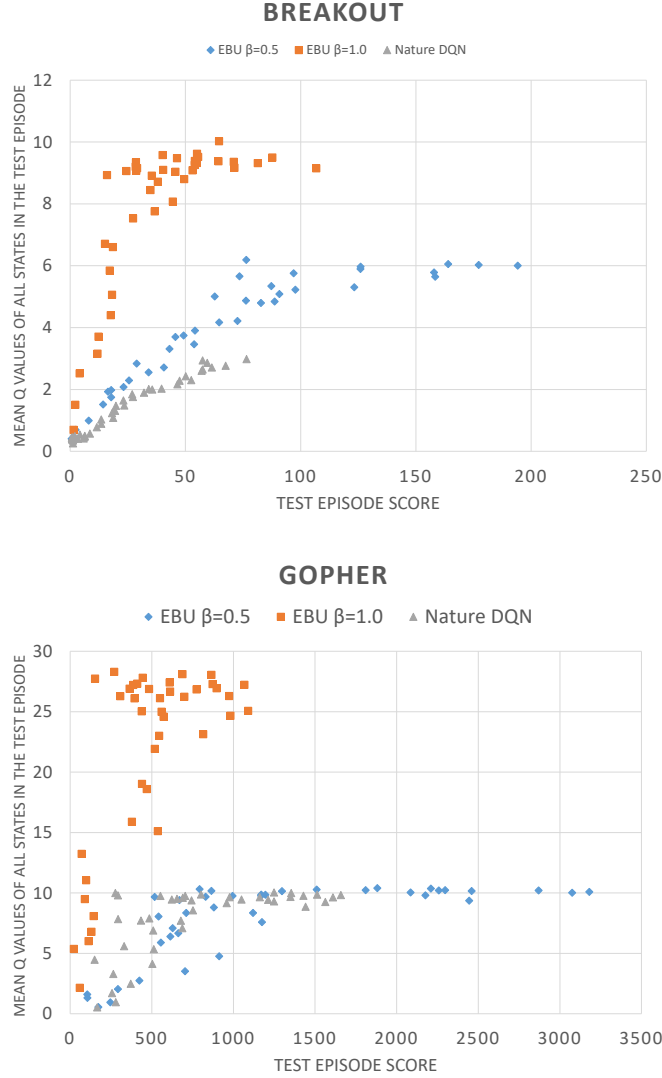


Figure 8: Test scores of episodes at the end of each epoch of training vs corresponding average Q-values of all state-action pairs.

EBU with $\beta = 1.0$ underperforms EBU with $\beta = 0.5$ in most of the Atari games that we tried. In order to analyze this phenomenon, we evaluate the Q-values learned by each agent at the end of each training epoch. At the end of each epoch, we test our agent and report the test episode score and the corresponding mean Q-values of transitions in the test episode (Figure 8).

We notice that the naive EBU with $\beta = 1.0$ is trained to output highly overestimated Q-values compared to its actual performance. Since EBU method performs recursive max operators at every updates, EBU outputs higher Q-values than Nature DQN. This result indicates that sequentially updating correlated states with overestimated values may destabilize the learning process. However, this result clearly implies that EBU with $\beta = 0.5$ is relatively free from the overestimation problem, and therefore performs safely and efficiently.

Appendix F Comparison to other Multi-step Methods.

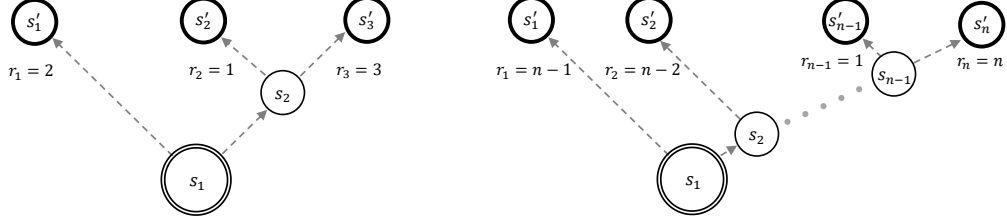


Figure 9: A motivating example where $Q(\lambda)$ underperforms Episodic Backward Update. **Left:** A simple navigation domain with 3 possible episodes. s_1 is the initial state. States with ' signs are the terminal states. **Right:** An extended example with n possible episodes.

Imagine a toy navigation environment as in Figure 9, left. Assume that an agent has experienced all possible trajectories: $(s_1 \rightarrow s'_1)$; $(s_1 \rightarrow s_2 \rightarrow s'_2)$ and $(s_1 \rightarrow s_2 \rightarrow s'_3)$. Let the discount factor γ be 1. Then optimal policy is $(s_1 \rightarrow s_2 \rightarrow s'_3)$. With a slight abuse of notation let $Q(s_i, s_j)$ denote the value of the action that leads to the state s_j from the state s_i . We will show that $Q(\lambda)$ and $Q^*(\lambda)$ methods underperform Episodic Backward Update in such examples with many suboptimal branching paths.

$Q(\lambda)$ method cuts trace of the path when the path does not follow greedy actions given current Q-value. For example, assume a $Q(\lambda)$ agent has updated the value $Q(s_1, s'_1)$ at first. When the agent tries to update the values of the episode $(s_1 \rightarrow s_2 \rightarrow s'_3)$, the greedy policy of the state s_1 heads to s'_1 . Therefore the trace of the optimal path is cut and the reward signal r_3 is not passed to $Q(s_1, s_2)$. This problem becomes more severe if the number of suboptimal branches increases as illustrated in Figure 9, right. Other variants of $Q(\lambda)$ algorithm that cut traces, such as Retrace(λ), have the same problem. EBU does not suffer from this issue, because EBU does not cut trace, but performs max operations at every branch to propagate the maximum value.

$Q^*(\lambda)$ is free from the issues mentioned above since it does not cut traces. However, to guarantee convergence to the optimal value function, it requires the parameter λ to be less than $\frac{1-\gamma}{2\gamma}$. In convention, the discount factor $\gamma \approx 1$. For a small value of λ that satisfies the constraint, the update of distant returns becomes nearly negligible. However, EBU does not have any constraint of the diffusion coefficient β to guarantee convergence.

Appendix G Theoretical Guarantees

Now, we will prove that the episodic backward update algorithm converges to the true action-value function Q^* in the case of finite and deterministic environment.

Definition 1. (*Deterministic MDP*)

$M = (S, A, P, R)$ is a **deterministic MDP** if $\exists g : S \times A \rightarrow S$ s.t.

$$P(s'|s, a) = \begin{cases} 1 & \text{if } s' = g(s, a) \\ 0 & \text{else} \end{cases} \quad \forall (s, a, s') \in S \times A \times S,$$

In the episodic backward update algorithm, a single (state, action) pair can be updated through multiple episodes, where the evaluated targets of each episode can be different from each other. Therefore, unlike the bellman operator, episodic backward operator depends on the exploration policy for the MDP. Therefore, instead of expressing different policies in each state, we define a schedule to represent the frequency of every distinct episode (which terminates or continues indefinitely) starting from the target (state, action) pair.

Definition 2. (*Schedule*)

Assume a MDP $M = (S, A, P, R)$, where R is a bounded function. Then, for each state $(s, a) \in S \times A$ and $j \in [1, \infty]$, we define **j -length path set** $p_{s,a}(j)$ and **path set** $p(s, a)$ for (s, a) as

$$p_{s,a}(j) = \{(s_i, a_i)_{i=0}^j | (s_0, a_0) = (s, a), P(s_{i+1}|s_i, a_i) > 0 \quad \forall i \in [0, j-1], s_j \text{ is terminal}\}.$$

and $p_{s,a} = \cup_{j=1}^{\infty} p_{s,a}(j)$.

Also, we define a **schedule set** $\lambda_{s,a}$ for (state action) pair (s, a) as

$$\lambda_{s,a} = \left\{ (\lambda_i)_{i=1}^{|p_{s,a}|} \mid \sum_{i=1}^{|p_{s,a}|} \lambda_i = 1, \lambda_i > 0 \quad \forall i \in [1, |p_{s,a}|] \right\}.$$

Finally, to express the varying schedule in time at the RL scenario, we define a **time schedule set** λ for MDP M as

$$\lambda = \left\{ \{\lambda_{s,a}(t)\}_{(s,a) \in S \times A, t=1}^{\infty} \mid \lambda_{s,a}(t) \in \lambda_{s,a} \quad \forall (s, a) \in S \times A, t \in [1, \infty] \right\}.$$

Since no element of the path can be the prefix of the others, the path set corresponds to the enumeration of all possible episodes starting from each (state, action) pair. Therefore, if we utilize multiple episodes from any given policy, we can see the empirical frequency for each path in the path set belongs to the schedule set. Finally, since the exploration policy can vary across time, we can group independent schedules into the time schedule set.

For a given time schedule and MDP, now we define the episodic backward operator.

Definition 3. (*Episodic backward operator*)

For an MDP $M = (S, A, P, R)$, and a time schedule $\{\lambda_{s,a}(t)\}_{t=1, (s,a) \in S \times A}^{\infty} \in \lambda$.

Then, the **episodic backward operator** H_t^β is defined as

$$(H_t^\beta Q)(s, a) \tag{5}$$

$$= \mathbb{E}_{s' \in S, P(s'|s, a)} \left[r(s, a, s') + \gamma \sum_{i=1}^{|p_{s,a}|} (\lambda_{(s,a)}(t))_i \mathbb{1}(s_{i1} = s') \left[\max_{1 \leq j \leq |(p_{s,a})_i|} T_{(p_{s,a})_i}^{\beta, Q}(j) \right] \right].$$

$$T_{(p_{s,a})_i}^{\beta, Q}(j) \tag{6}$$

$$= \sum_{k=1}^{j-1} \beta^{k-1} \gamma^{k-1} \{ \beta r(s_{ik}, a_{ik}, s_{i(k+1)}) + (1 - \beta) Q(s_{ik}, a_{ik}) \} + \beta^{j-1} \gamma^{j-1} \max_{a \neq a_j} Q(s_{ij}, a_{ij}).$$

Where $(p_{s,a})_i$ is the i -th path of the path set, and (s_{ij}, a_{ij}) corresponds to the j -th (state, action) pair of the i -th path.

Episodic backward operator consists of two parts. First, given the path that initiates from the target (state, action) pair, function $T_{(p_{s,a})_i}^{\beta, Q}$ computes the maximum return of the path via backward update. Then, the return is

averaged by every path in the path set. Now, if the MDP M is deterministic, we can prove that the episodic backward operator is a contraction in the sup-norm, and the fixed point of the episodic backward operator is the optimal action-value function of the MDP regardless of the time schedule.

Theorem 2. (Contraction of episodic backward operator and the fixed point)

Suppose $M = (S, A, P, R)$ is a deterministic MDP. Then, for any time schedule $\{\lambda_{s,a}(t)\}_{t=1, (s,a) \in S \times A}^\infty \in \lambda$, H_t^β is a contraction in the sup-norm for any t , i.e

$$\|(H_t^\beta Q_1) - (H_t^\beta Q_2)\|_\infty \leq \gamma \|Q_1 - Q_2\|_\infty. \quad (7)$$

Furthermore, for any time schedule $\{\lambda_{s,a}(t)\}_{t=1, (s,a) \in S \times A}^\infty \in \lambda$, the fixed point of H_t^β is the optimal Q function Q^* .

Proof. First, we prove $T_{(p_{s,a})_i}^{\beta, Q}(j)$ is a contraction in the sup-norm for all j .

Since M is a deterministic MDP, we can reduce the return as

$$T_{(p_{s,a})_i}^{\beta, Q}(j) = \left(\sum_{k=1}^{j-1} \beta^{k-1} \gamma^{k-1} \{ \beta r(s_{ik}, a_{ik}) + (1-\beta)Q(s_{ik}, a_{ik}) \} + \beta^{j-1} \gamma^{j-1} \max_{a \neq a_j} Q(s_{ij}, a_{ij}) \right). \quad (8)$$

$$\begin{aligned} \|T_{(p_{s,a})_i}^{\beta, Q_1}(j) - T_{(p_{s,a})_i}^{\beta, Q_2}(j)\|_\infty &\leq \left\{ (1-\beta) \sum_{k=1}^{j-1} \beta^{k-1} \gamma^{k-1} + \beta^{j-1} \gamma^{j-1} \right\} \|Q_1 - Q_2\|_\infty \\ &= \left\{ \frac{(1-\beta)(1-(\beta\gamma)^{j-1})}{1-\beta\gamma} + \beta^{j-1} \gamma^{j-1} \right\} \|Q_1 - Q_2\|_\infty \\ &= \frac{1-\beta + \beta^j \gamma^{j-1} - \beta^j \gamma^j}{1-\beta\gamma} \|Q_1 - Q_2\|_\infty \\ &= \left\{ 1 + (1-\gamma) \frac{\beta^j \gamma^{j-1} - \beta}{1-\beta\gamma} \right\} \|Q_1 - Q_2\|_\infty \\ &\leq \|Q_1 - Q_2\|_\infty (\because \beta \in [0, 1], \gamma \in [0, 1)). \end{aligned} \quad (9)$$

Also, at the deterministic MDP, the episodic backward operator can be reduced to

$$(H_t^\beta Q)(s, a) = r(s, a) + \gamma \sum_{i=1}^{|p_{s,a}|} (\lambda_{(s,a)}(t))_i \left[\max_{1 \leq j \leq |p_{s,a}|} T_{(p_{s,a})_i}^{\beta, Q}(j) \right]. \quad (10)$$

Therefore, we can finally conclude that

$$\begin{aligned}
& \| (H_t^\beta Q_1) - (H_t^\beta Q_2) \|_\infty \\
&= \max_{s,a} \left| H_t^\beta Q_1(s,a) - H_t^\beta Q_2(s,a) \right| \\
&\leq \gamma \max_{s,a} \left[\sum_{i=1}^{|p_{s,a}|} (\lambda_{(s,a)}(t))_i \left| \left\{ \max_{1 \leq j \leq |p_{s,a}|} T_{(p_{s,a})_i}^{\beta, Q_1}(j) \right\} - \left\{ \max_{1 \leq j \leq |p_{s,a}|} T_{(p_{s,a})_i}^{\beta, Q_2}(j) \right\} \right| \right] \\
&\leq \gamma \max_{s,a} \left[\sum_{i=1}^{|p_{s,a}|} (\lambda_{(s,a)}(t))_i \max_{1 \leq j \leq |p_{s,a}|} \left\{ \left| T_{(p_{s,a})_i}^{\beta, Q_1}(j) - T_{(p_{s,a})_i}^{\beta, Q_2}(j) \right| \right\} \right] \\
&\leq \gamma \max_{s,a} \left[\sum_{i=1}^{|p_{s,a}|} (\lambda_{(s,a)}(t))_i \|Q_1 - Q_2\|_\infty \right] \\
&= \gamma \max_{s,a} [\|Q_1 - Q_2\|_\infty] \\
&= \gamma \|Q_1 - Q_2\|_\infty.
\end{aligned} \tag{11}$$

Therefore, we proved that episodic backward operator is a contraction independent of the schedule. Finally, we prove that the distinct episodic backward operators in terms of schedule has same fixed point, Q^* . A sufficient condition to prove this is given by

$$\left[\max_{1 \leq j \leq |p_{s,a}|} T_{(p_{s,a})_i}^{\beta, Q^*}(j) \right] = \frac{Q^*(s,a) - r(s,a)}{\gamma} \quad \forall 1 \leq i \leq |p_{s,a}|.$$

We will prove this by contradiction. Assume $\exists i$ s.t. $\left[\max_{1 \leq j \leq |p_{s,a}|} T_{(p_{s,a})_i}^{\beta, Q^*}(j) \right] \neq \frac{Q^*(s,a) - r(s,a)}{\gamma}$.

First, by the definition of Q^* fuction, we can bound $Q^*(s_{ik}, a_{ik})$ and $Q^*(s_{ik}, :)$ for every $k \geq 1$ as follows.

$$Q^*(s_{ik}, a) \leq \gamma^{-k} Q^*(s, a) - \sum_{m=0}^{k-1} \gamma^{m-k} r(s_{im}, a_{im}). \tag{12}$$

Note that the equality holds if and only if the path $(s_i, a_i)_{i=0}^{k-1}$ is the optimal path among the ones that start from (s_0, a_0) . Therefore, $\forall 1 \leq j \leq |p_{s,a}|$, we can bound $T_{(p_{s,a})_i}^{\beta, Q^*}(j)$.

$$\begin{aligned}
& T_{(p_{s,a})_i}^{\beta, Q}(j) \\
&= \sum_{k=1}^{j-1} \beta^{k-1} \gamma^{k-1} \{ \beta r(s_{ik}, a_{ik}) + (1-\beta) Q(s_{ik}, a_{ik}) \} + \beta^{j-1} \gamma^{j-1} \max_{a \neq a_j} Q(s_{ij}, a_{ij}) \\
&\leq \left\{ \left(\sum_{k=1}^{j-1} (1-\beta) \beta^{k-1} \right) + \beta^{j-1} \right\} \gamma^{-1} Q^*(s, a) \\
&\quad + \sum_{k=1}^{j-1} \left\{ \beta^{k-1} \gamma^{k-1} \left(\beta r(s_{ik}, a_{ik}) - \sum_{m=0}^{k-1} (1-\beta) \gamma^{m-k} r(s_{im}, a_{im}) \right) \right\} \\
&\quad - \sum_{m=0}^{j-1} \beta^{j-1} \gamma^{j-1} \gamma^{m-j} r(s_{im}, a_{im}) \\
&= \gamma^{-1} Q^*(s, a) + \sum_{k=1}^{j-1} \beta^k \gamma^{k-1} r(s_{ik}, a_{ik}) \\
&\quad - \sum_{m=0}^{j-2} \left\{ \sum_{k=m+1}^{j-1} (1-\beta) \beta^{k-1} \gamma^{m-1} r(s_{im}, a_{im}) \right\} - \sum_{m=0}^{j-1} \beta^{j-1} \gamma^{m-1} r(s_{im}, a_{im}) \\
&= \gamma^{-1} Q^*(s, a) + \sum_{m=1}^{j-1} \beta^m \gamma^{m-1} r(s_{im}, a_{im}) \\
&\quad - \sum_{m=0}^{j-2} (\beta^m - \beta^{j-1}) \gamma^{m-1} r(s_{im}, a_{im}) - \sum_{m=0}^{j-1} \beta^{j-1} \gamma^{m-1} r(s_{im}, a_{im}) \\
&= \gamma^{-1} Q^*(s, a) - \gamma^{-1} r(s_{i0}, a_{i0}) = \frac{Q^*(s, a) - r(s, a)}{\gamma}.
\end{aligned} \tag{13}$$

Since this occurs for any arbitrary path, the only remaining case is when

$$\exists i \text{ s.t. } \left[\max_{1 \leq j \leq |(p_{s,a})_i|} T_{(p_{s,a})_i}^{\beta, Q^*}(j) \right] < \frac{Q^*(s, a) - r(s, a)}{\gamma}.$$

Now, let's speculate on the path $s_0, s_1, s_2, \dots, s_{|(p_{s,a})_i|}$. Let's first prove the contradiction when the length of the contradictory path is finite. If $Q^*(s_{i1}, a_{i1}) < \gamma^{-1}(Q^*(s, a) - r(s, a))$, then by the bellman equation, there exists action $a \neq a_{i1}$ s.t $Q^*(s_{i1}, a) = \gamma^{-1}(Q^*(s, a) - r(s, a))$. Then, we can find that $T_{(p_{s,a})_1}^{\beta, Q^*}(1) = \gamma^{-1}(Q^*(s, a) - r(s, a))$ so it contradicts the assumption. Therefore, a_{i1} should be the optimal action in s_{i1} .

Repeating the procedure, we can find that $a_{i1}, a_{i2}, \dots, a_{|(p_{s,a})_i|-1}$ are optimal with respect to their corresponding states.

Finally, we can find that $T_{(p_{s,a})_1}^{\beta, Q^*}(|(p_{s,a})_i|) = \gamma^{-1}(Q^*(s, a) - r(s, a))$ since all the actions satisfies the optimality condition of the inequality in equation 7. Therefore, it is a contradiction to the assumption.

In the case of infinite path, we will prove that for any $\epsilon > 0$, there is no path that satisfy $\frac{Q^*(s, a) - r(s, a)}{\gamma} - \left[\max_{1 \leq j \leq |(p_{s,a})_i|} T_{(p_{s,a})_i}^{\beta, Q^*}(j) \right] = \epsilon$.

Since the reward function is bounded, we can define r_{\max} as the supremum norm of the reward function. Define $q_{\max} = \max_{s,a} |Q(s, a)|$ and $R_{\max} = \max\{r_{\max}, q_{\max}\}$. We can assume $R_{\max} > 0$. Then, let's set $n_\epsilon = \lceil \log_\gamma \frac{\epsilon(1-\gamma)}{R_{\max}} \rceil + 1$. Since $\gamma \in [0, 1)$, $R_{\max} \frac{\gamma^{n_\epsilon}}{1-\gamma} < \epsilon$. Therefore, by applying the procedure on the finite path case for $1 \leq j \leq n_\epsilon$, we can conclude that the assumption leads to a contradiction. Since the previous n_ϵ trajectories are optimal, the rest trajectories can only generate a return less than ϵ .

Finally, we proved that $\left[\max_{1 \leq j \leq |(p_{s,a})_i|} T_{(p_{s,a})_i}^{\beta, Q^*}(j) \right] = \frac{Q^*(s,a) - r(s,a)}{\gamma} \forall 1 \leq i \leq |p_{s,a}|$ and therefore, every episodic backward operator has Q^* as the fixed point. \square

Finally, we will show that the online episodic backward update algorithm converges to the optimal Q function Q^* .

Restatement of Theorem 1. *Given a finite, deterministic, and tabular MDP $M = (S, A, P, R)$, the episodic backward update algorithm, given by the update rule*

$$Q_{t+1}(s_t, a_t) = (1 - \alpha_t)Q_t(s_t, a_t) + \alpha_t \left[r(s_t, a_t) + \gamma \sum_{i=1}^{|p_{s_t, a_t}|} (\lambda_{(s_t, a_t)})_i(t) \left[\max_{1 \leq j \leq |(p_{s_t, a_t})_i|} T_{(p_{s_t, a_t})_i}^{\beta, Q}(j) \right] \right] \text{ converges to the optimal } Q \text{ function w.p. 1 as long as}$$

- The step size satisfies the Robbins-Monro condition;
- The sample trajectories are finite in lengths l : $\mathbb{E}[l] < \infty$;
- Every (state, action) pair is visited infinitely often.

For the proof of Theorem 1, we follow the proof of [Melo, 2001](#).

Lemma 1. *The random process Δ_t taking values in \mathbb{R}^n and defined as*

$$\Delta_{t+1}(x) = (1 - \alpha_t(x))\Delta_t(x) + \alpha_t(x)F_t(x)$$

converges to zero w.p.1 under the following assumptions:

- $0 \leq \alpha_t \leq 1$, $\sum_t \alpha_t(x) = \infty$ and $\sum_t \alpha_t^2(x) < \infty$;
- $\|\mathbb{E}[F_t(x)|\mathcal{F}_t]\|_W \leq \gamma \|\Delta_t\|_W$, with $\gamma < 1$;
- $\text{var}[F_t(x)|\mathcal{F}_t] \leq C(1 + \|\Delta_t\|_W^2)$, for $C > 0$.

By Lemma 1, we can prove that the online episodic backward update algorithm converges to the optimal Q^* .

Proof. First, by assumption, the first condition of Lemma 1 is satisfied. Also, we can see that by substituting $\Delta_t(s, a) = Q_t(s, a) - Q^*(s, a)$, and $F_t(s, a) = r(s, a) + \gamma \sum_{i=1}^{|p_{s,a}|} (\lambda_{(s,a)})_i(t) \left[\max_{1 \leq j \leq |(p_{s,a})_i|} T_{(p_{s,a})_i}^{\beta, Q}(j) \right] - Q^*(s, a)$. $\|\mathbb{E}[F_t(s, a)|\mathcal{F}_t]\|_\infty = \|(H_t^\beta Q_t)(s, a) - (H_t^\beta Q^*)(s, a)\|_\infty \leq \gamma \|\Delta_t\|_\infty$, where the inequality holds due to the contraction of the episodic backward operator.

$$\text{Then, } \text{var}[F_t(x)|\mathcal{F}_t] = \text{var} \left[r(s, a) + \gamma \sum_{i=1}^{|p_{s,a}|} (\lambda_{(s,a)})_i(t) \left[\max_{1 \leq j \leq |(p_{s,a})_i|} T_{(p_{s,a})_i}^{\beta, Q}(j) \right] \middle| \mathcal{F}_t \right].$$

Since the reward function is bounded, the third condition also holds as well. Finally, by Lemma 1, Q_t converges to Q^* . \square

Although the episodic backward operator can accommodate infinite paths, the operator can be practical when the maximum length of the episode is finite. This assumption holds for many RL domains, such as ALE.